SEISMIC SOIL PRESSURES ON EMBEDDED WALLS WITH VARYING STIFFNESS AND CONTACT CONDITIONS[1]

Andrea E. Cruz-Chamorro[2], Aidcer L. Vidot-Vega[3]

ABSTRACT: This article evaluates how the seismic pressures developed in embedded walls are affected by different wall stiffness and various contact soil-wall conditions. Several two-dimensional numerical models of an embedded wall-soil system were developed in Abaqus® by varying the wall stiffness. One model considered the wall as very rigid with a large modulus of elasticity and the other one considered the wall as flexible with original modulus of elasticity. Wall heights of 10, 20 and 30 meters were considered on the models to obtain different wall stiffness. The contact between the soil and the wall is modified by changing the friction coefficient between 0 to 0.75. The response of the soil is validated using 1D nonlinear site response analyses. The analyses are performed using records that match a narrow-band modified target spectrum for a moment magnitude of 7.70. The results show that the rigid walls developed larger seismic pressures than the flexible walls when subjected to the same earthquake records. The seismic soil pressures in the rigid walls do not change considerably by varying the contact condition between the soil and wall. Changes in the friction coefficient have a major impact on the seismic pressure distributions on flexible walls.

Keywords: contact, embedded walls, friction, seismic pressures, wall stiffness

PRESIONES SÍSMICAS DEL SUELO EN MUROS ENTERRADOS CON RIGIDECES Y CONDICIONES DE CONTACTO VARIABLES

RESUMEN: Este artículo evalúa cómo las presiones sísmicas desarrolladas en muros enterrados en la tierra se ven afectadas por diferentes rigideces de muros y diversas condiciones de contacto suelo-muro. En Abaqus® se desarrollaron varios modelos numéricos en dos dimensiones de un sistema pared enterrada y suelo variando la rigidez de la pared. Un modelo consideró la pared como muy rígida con un módulo de elasticidad bien grande y el otro consideró la pared como flexible con módulo de elasticidad original. En los modelos se consideraron alturas de pared de 10, 20 y 30 m para obtener diferentes rigideces de pared. El contacto entre el suelo y la pared se modifica cambiando el coeficiente de fricción entre 0 y 0.75. La respuesta del suelo se valida mediante análisis de respuesta de sitio no lineales en una dimensión. Los análisis se realizan utilizando registros que coinciden con un espectro modificado de banda estrecha para una magnitud de momento de 7.70. Los resultados muestran que los muros rígidos desarrollaron mayores presiones sísmicas que los muros flexibles cuando se sometieron a los mismos registros sísmicos. Las presiones sísmicas del suelo en los muros rígidos no cambian considerablemente al variar la condición de contacto entre el suelo y el muro. Los cambios en el coeficiente de fricción tienen un gran impacto en las distribuciones de presión sísmica en las paredes flexibles.

Palabras claves: contacto, paredes enterradas, fricción, presiones sísmicas, rigidez de pared

INTRODUCTION

According to the World Nuclear Association (WNA), there are 439 nuclear reactors in operation in 30 countries around the world. The United States had the largest number of nuclear power reactors in operation at the time (92 units). France gets around 70% of its electricity from nuclear energy. However, in Latin America there are only seven nuclear power reactors in operation, producing just 2.2% of total energy consumption in Latin America. From these reactors, three are in Argentina, two in Brazil and two in Mexico (WNA, 2021). WNA also estimated that 20% of the operating nuclear reactors are located in earthquake

[1] Article received on March 20, 2023 and accepted for publication on April 25, 2023.
[2] PhD Candidate, Dept. of Civil Engineering and Surveying, University of Puerto Rico, Mayagüez, Puerto Rico 00681. Email: andrea.cruz1@upr.edu
[3] Professor, Dept. of Engineering Sciences and Materials, University of Puerto Rico, Mayagüez, Puerto Rico. Email: aidcer.vidot@upr.edu

hazard zones. Seismic analyses of nuclear power plants are important to determine appropriate design actions that ensure the safety integrity of all elements during a major earthquake event. Most of the nuclear power plant buildings are partially or deeply embedded in soil requiring the incorporation of soil-structure interaction (SSI) effects in the analyses. Therefore, to obtain a more accurate result, it is recommended to consider SSI effects, taking into consideration that both systems will not necessarily act as completely bonded during an earthquake event. In estimating the seismic induced soil pressure, an important consideration, and a real challenge in developing the SSI model is how to represent the structure-soil interface as close as possible to the real situation (Xu et al., 2006). The numerical modelling of the contact between soil and structures at the interface is key to obtaining realistic solutions for the response of the soil structure interaction system (Datta et al., 2018). Therefore, the objective of this article is to study how the soil-wall interaction is affected by different contact friction conditions during an earthquake event. SSI effects in induced seismic pressures are considered in several soil-wall finite element models by varying the coefficient of friction at the interface. All the results are compared with a bonded soil-wall case.

FINITE ELEMENT MODELS

Two-dimensional finite element models of embedded wall–soil systems were developed in Abaqus®. One of the models considered the wall as very rigid with a large modulus of elasticity (1000*E) and the other one considered the wall as flexible with original modulus of elasticity (E). The densities of the wall material and soil were 2,400 kg/m^3 and 2,200 kg/m^3, respectively. The Poisson's coefficients of the wall material and soil were 0.20 and 0.25, respectively. The pressure-dependent hyperbolic model (MKZ) developed by Matasovic (1993), which is a modification of the model by Konder and Zelasko (1963), was used to model the nonlinear behavior of the soil and to obtain the backbone curve for the analyses. The equation for the shear strength of the backbone curve is presented in equation (1) varying the value of the shear strain (equation 2). For this case, the shear wave velocity of the soil deposit is 350 m/s. The parameters used for the soil in the finite element analyses performed in this work are for granular soil (sand) with no water and no liquefaction in the soil. If liquefaction of soil is expected, the results of these analyses can vary significantly. The rock was considered as an elastic and linear material, with a shear wave velocity of 1800 m/s. Table 1 shows all the material properties used in the analyses. Table 2 shows the properties of the walls in the models. Figure 1 shows an example of how the backbone curve behaves when varying the β parameter, showing that the smaller the variable is, the larger shear strength is reached.

Table 1: **Soil and rock properties**.

	Soil	**Rock**
Density ρ (kg/m$^{3)}$	2200	2800
Poisson's ratio ν	0.25	0.3
Shear Modulus G_o (MPa	269.5	9072
S	0.6	-
γ_r	0.0003	-
β	0.85	-
σ_{ref} [MPa]	0.20	-

Table 2: Flexible and rigid wall properties.

	Flexible Wall	Rigid Wall (1000*E)
Density ρ [kg/m^3]	2400	2400
Poisson's ratio *v*	0.2	0.2
Compressive strength *f'c* [*MPa*]	28	28
Young Modulus *E* [*MPa*]	24870.06	24870062.32

A built-in user material available in the Abaqus 2016 version was used for the hysteretic soil model including the backbone obtained from the MKZ model (Figure 1). This option allows to simulate the response of the soil under seismic loads (ABQ_HYST_SOIL). A characteristic of this material is that it is similar to the MAT_079 material in LS_DYNA. This model is a nested surface model that incorporates up to ten layers of elasto-perfectly plastic material. The hysteretic behavior is generated by superimposing various layers of the material. The value of stress at any instant is the sum of the stresses at each individual layer, resulting in a piecewise-linear backbone. This curve is broken into ten layers each having a value of elastic moduli and yield stress (Bolisetti and Whittaker, 2015). These properties are pressure dependent and are described by Equations 3 to 4. The values for the different hysteretic material parameters are the following: b (exponent for pressure-sensitive moduli) = 0, yield constants $a_0 = 0$, $a_1 = 0$, and $a_2 = 1$. These values represent typical values for this type of analysis.

$$\tau = \frac{G_0\,\gamma}{1 + \beta\left(\frac{\gamma}{\gamma_r}\right)^s} \tag{1}$$

$$\gamma_r = \gamma_{ref}\left(\frac{\sigma'_v}{\sigma_r}\right)^b \tag{2}$$

Where,

τ = shear strength
G_0 = initial shear modulus
γ = shear strain
γ_r= reference shear strain
γ_{ref} = reference shear strain at the reference pressure

σ_r = reference shear stress
σ'_v= effective vertical stress
β and s = stress-strain curve parameter
b = pressure dependent parameter

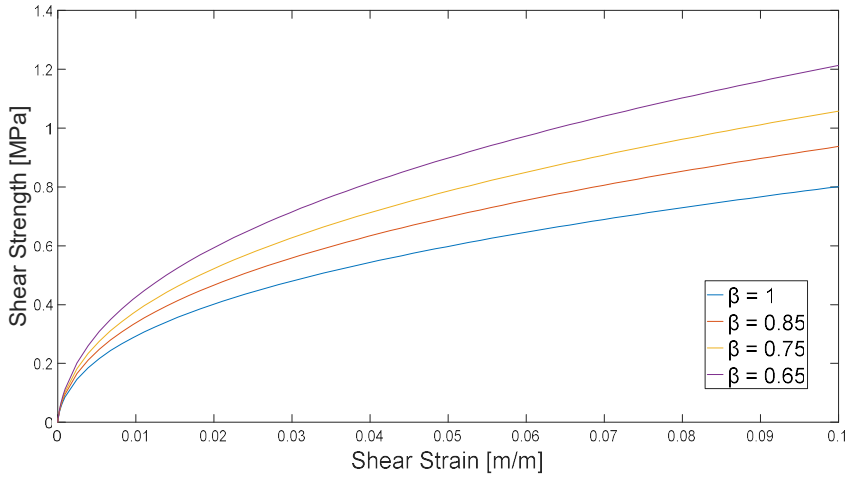

Figure 1: Pressure-Dependent Hyperbolic Model Backbone Curve

$$G(p) = \frac{G_r(p - p_0)^b}{(p_{ref} - p_0)^b} \tag{3}$$

$$\frac{\tau(p)}{\tau(p_{ref})} = \sqrt{\frac{a_0 + a_1(p - p_0) + a_2(p - p_0)^2}{a_0 + a_1(p_{ref} - p_0) + a_2(p_{ref} - p_0)^2}} \tag{4}$$

G_r = is the shear modulus at the layer of reference pressure

p= current pressure

p_0 = cut-off pressure. This value must be less than zero to withstand tension = -1e6

p_{ref} = reference pressure of the backbone curve

$\tau(p_{ref})$ = yield stress of the layer at reference pressure

$\tau(p)$ = yield stress of the layer at pressure p

The friction coefficient in the finite element models varied from 0 to 0.75 considering the Coulomb friction model. These values correspond to friction angles between 14 to 37 degrees. Three different wall heights were considered in this study (10m, 20m and 30m). Solid elements of 8 nodes with incompatible modes (C3D8I) were chosen for the wall because they can model its response accurately by improving the bending behavior (Abaqus, 2016). Figure 2 shows the finite element of the soil-wall system in Abaqus and the soil-column model developed to validate the results from the program. In the left of the model (Figure 2b), the element length is 4 times the length of the rest of the elements. This part of the model is used to simulate the free field behavior. The length of each element in each direction (dx and dy) was set to 2m. Constraints were assigned to the black nodes in the x and z direction in order to have the same displacement during the analysis. Likewise, constraints were assigned to all the nodes of the finite element model to have the same displacement in the y direction and consequently avoid warping deformations. Displacements out of plane (y-direction) are also constrained because the Abaqus/Explicit soil model consists of solid elements for rock and soil causing the model to be considered in 3D to assign the hysteretic material to the soil

elements. Three dashpots were incorporated at the base to model absorbing boundary conditions for the wave propagation. This finite element model is based on the one developed by Luna-Tezna et al. (2018) to study analytical seismic pressures in rigid retaining walls comparing them with simplified pressure approaches used in engineering practice. The method developed by Lysmer-Kuhlemeyer (1969) was used to calculate the dashpot coefficient (c_h and c_v) in the different directions. Equation 5 calculates the coefficient for the x and y directions, and equation 6 for the z (vertical) direction. The properties used in the damping calculations are shown in Tables 1 and 2.

$$c_h = A_{rock}\sqrt{G_{rock} * \rho_{rock}} \tag{5}$$

$$c_v = A_{rock}\sqrt{E_p * \rho_{rock}} \tag{6}$$

where:
A_{rock} = surface area of the rock in the horizontal direction.
G_{rock} = rock shear modulus
ρ_{rock} = rock density
E_p = normal stiffness rock modulus = (2ν-2)/(2ν-1) G_{rock}

The model was validated with one-dimensional nonlinear site response analyses (Figure 2a) using DeepSoil (Hashash et al., 2016) and compared with the response obtained of a soil-column model in Abaqus® (Figure 2b). The first model that was developed in ABAQUS does not include the wall in order to validate the results of the soil model used in the analyses. Figure 3 shows the accelerations and relative velocity results of the soil-column models developed from both programs. They show that results agree with each other. These results were obtained using a ground motion record from Northridge Earthquake (M_w= 6.7) scaled to 0.7g. Figure 4 shows the shear stress vs strain hysteretic results for an element in the bottom of the model between the soil and rock together with the backbone curve (showing only one direction). Shear strains are lower than 0.1% considered in the range of small deformations. The agreement of both program responses gave confidence to include the wall in the soil model in ABAQUS (Figure 2b).

Three non-pulse like earthquake ground records with a moment magnitude of 7.70 were used for the rest of the analyses with the soil-wall model. Non-pulse-like ground motions were obtained from a study performed by Roman-Velez and Montejo (2020). They took the task of generating 1624 compatible ground motions that would match the seven target spectra of moderate to strong magnitude earthquakes. From the NGA-West2 database they obtained the seed records (Ancheta et al., 2013). Figure 5 shows the acceleration time histories with the pseudo acceleration and velocity response spectrums of these earthquakes.

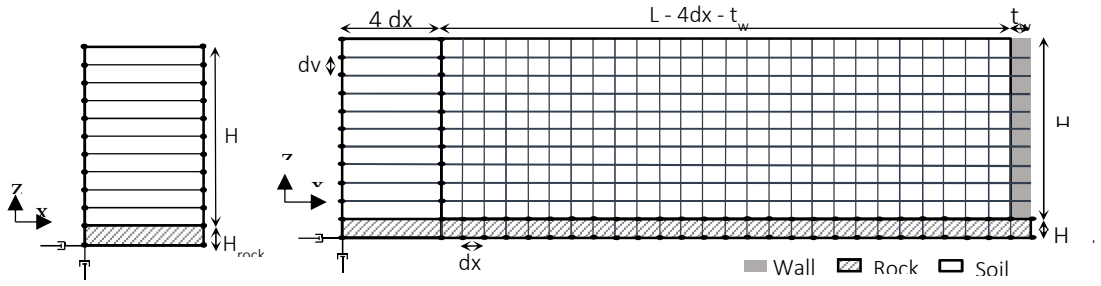

Figure 2: **a) Finite element model soil column. b) Soil – wall finite element model**. **(Luna-Tezna et al. 2018)**

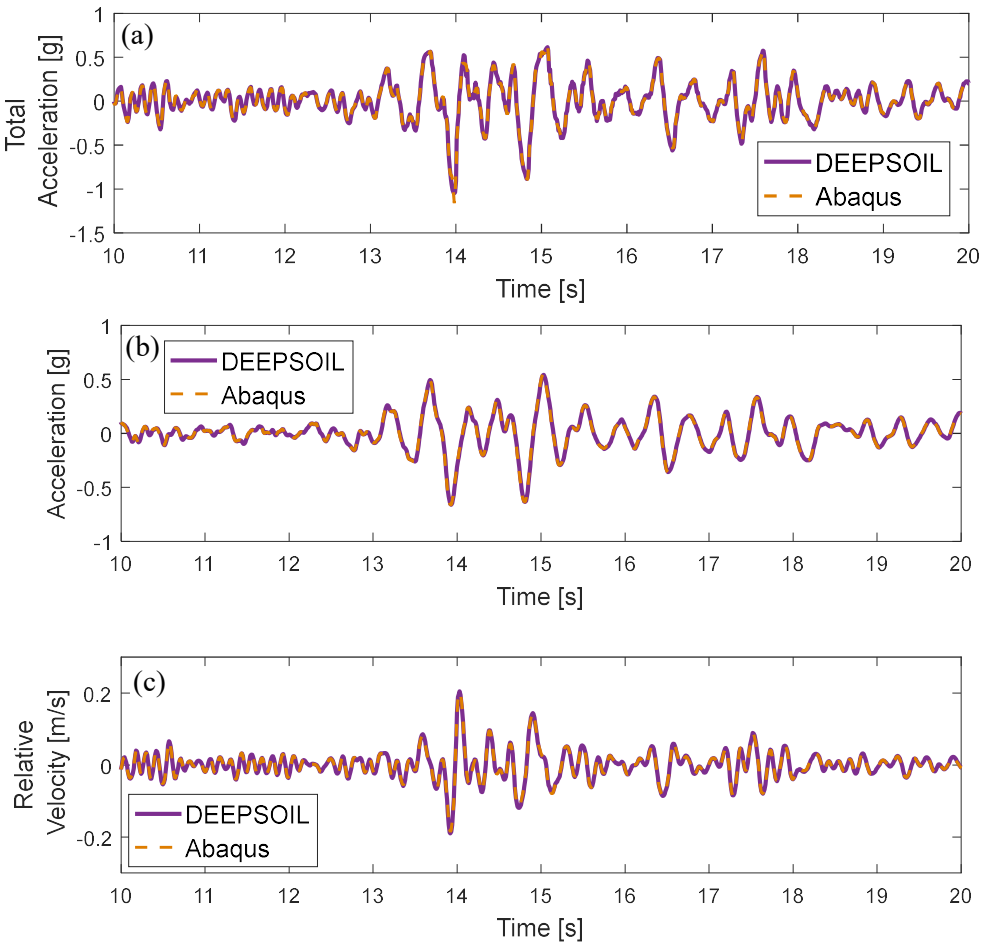

Figure 3: **(a)Total acceleration at the soil surface, (b) total acceleration at the rock surface, (c) relative velocity at the soil surface.**

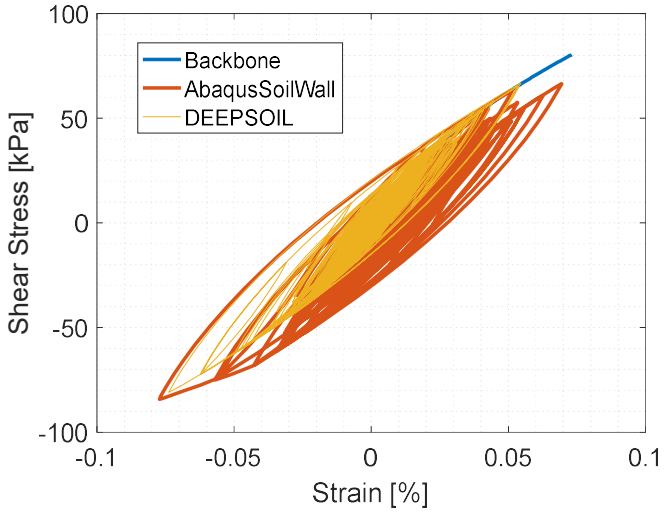

Figure 4: **Example of shear Stress vs shear strain for an element between rock and soil.**

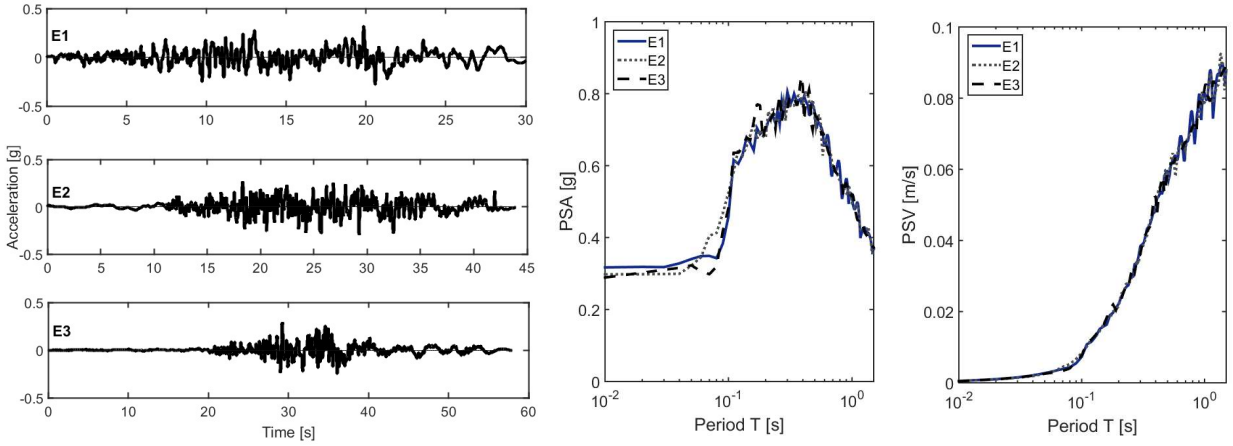

Figure 5: **Acceleration time histories and pseudo acceleration and velocity response spectrums.**

FINITE ELEMENT ANALYSIS RESULTS

This section presents the results obtained from the finite element models of the soil-wall system developed in Abaqus for different friction contact conditions, different modulus of elasticity (original-flexible and rigid) and three heights (10m, 20m and 30m). The average normalized seismic soil pressures obtained from the three earthquake records are shown in Figures 6-8. These figures show the normalized pressures that were obtained by dividing pressures by the unit weight of the soil (γ) and height (H) of the wall. On the vertical graph axis, the distances are normalized with respect to the wall's height. The pressures are considered positive when they induce compression on the wall. These figures presented the results obtained using five different contact conditions (bonded and with friction coefficients 0, 0.25, 0.50, 0.75). The rigid case considered the wall with a large modulus of elasticity. The flexible case is the wall with the original modulus of elasticity. The seismic soil pressures developed in the wall shown in these figures were obtained when the maximum base shear occurs in the wall.

The distribution of the average seismic pressures varied considerably when the wall is rigid or flexible. As the height of the wall increases, the change in pressure distribution is more noticeable. Psarropoulos et al. (2005) studied the seismic pressures distributions in rigid and flexible walls noticing these changes in pressure distributions. They observed that for relatively rigid systems there is a sinusoidal-like increase of the pressures from the base to the top of the wall. They noticed that for more flexible systems, the maximum pressures occur closer to the base. Wagner and Sitar (2016) also showed that the flexibility of the retaining structures plays a very important role in the magnitude of the predicted seismic loads and pressures and that their magnitude significantly decreases with increased wall flexibility considering a perfectly bonded condition. Similar, Luna et. al (2018) identified that the magnitude of the pressures varies depending on the stiffness of the wall. However, the effect of different contact conditions was not included in any of these investigations.

Figures 9-10 present the comparison of the normalized seismic soil pressures obtained for the different friction case scenarios as function of the normalized wall height for flexible and rigid wall cases, respectively. Nevertheless, the change in the friction coefficient between the soil and the wall has less effect in seismic pressure distributions than the flexibility condition. For the flexible wall with 30 m, there are mayor changes in seismic pressure distributions when the contact condition based on the friction coefficient is varied. In general, the seismic pressures are similar for friction coefficients 0.5 and 0.75. This range is within typical friction coefficients used in soil-wall interaction analyses. A friction coefficient of 0.7

corresponds to a 35-degree friction angle which is reasonable for typical soil used as backfills (Xu et al., 2006). According to these results, seems that the variability in seismic soil pressures in embedded walls is increased by wall flexibility and friction contact conditions.

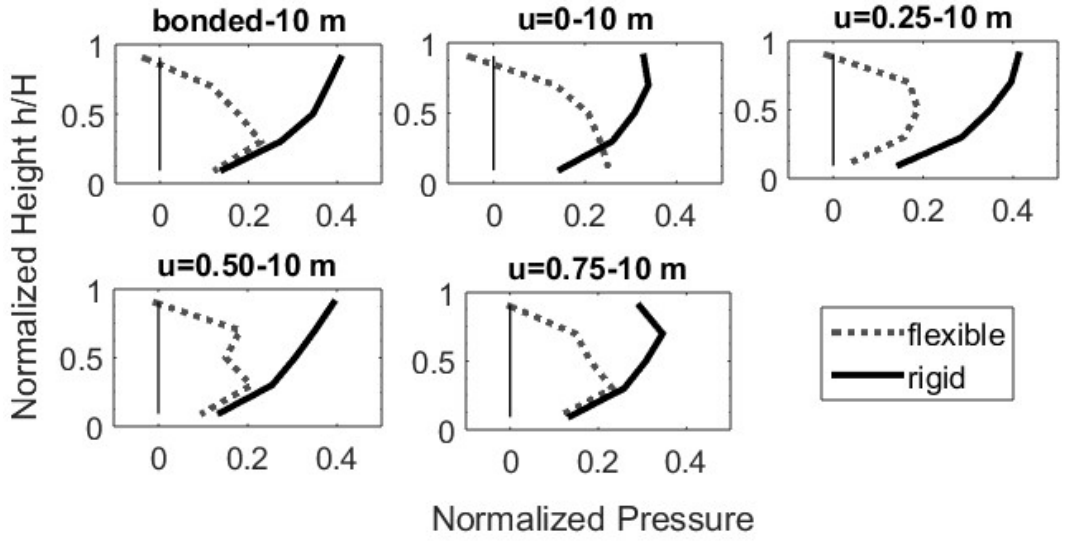

Figure 6: **Normalized seismic pressures for rigid vs. flexible walls with height of 10 m**.

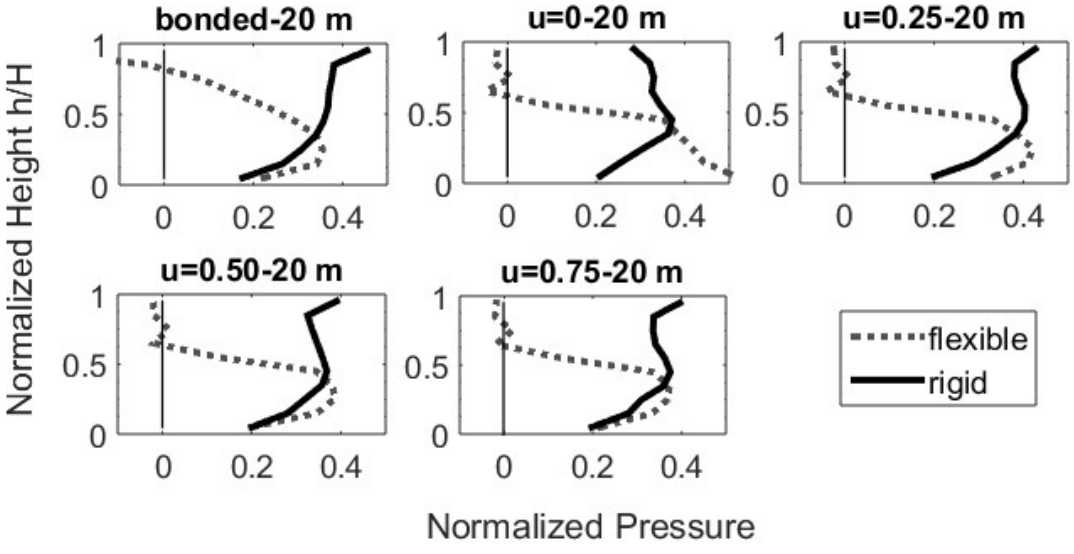

Figure 7: Normalized seismic pressures for rigid vs. flexible walls with height of 20 m.

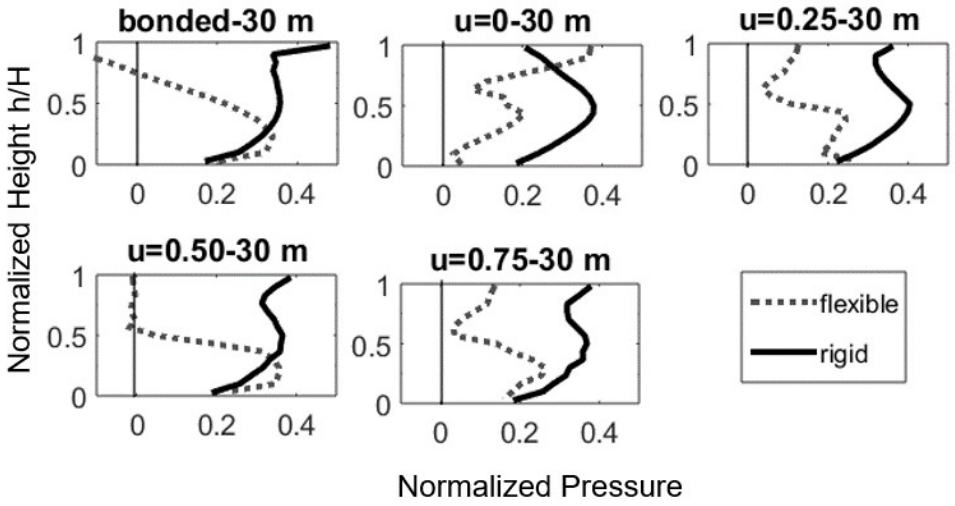

Figure 8: **Normalized seismic pressures for rigid vs. flexible walls with height of 30 m**.

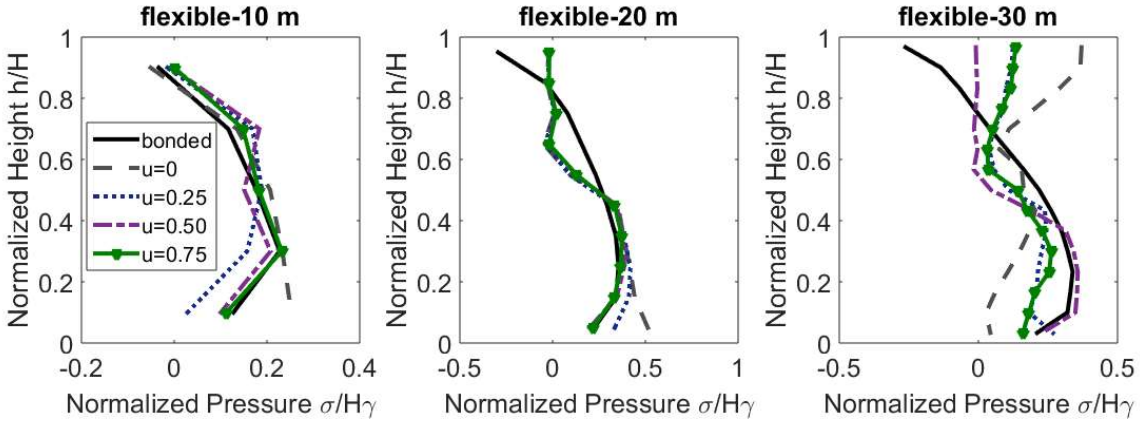

Figure 9: **Normalized seismic pressures for flexible walls (original E)**.

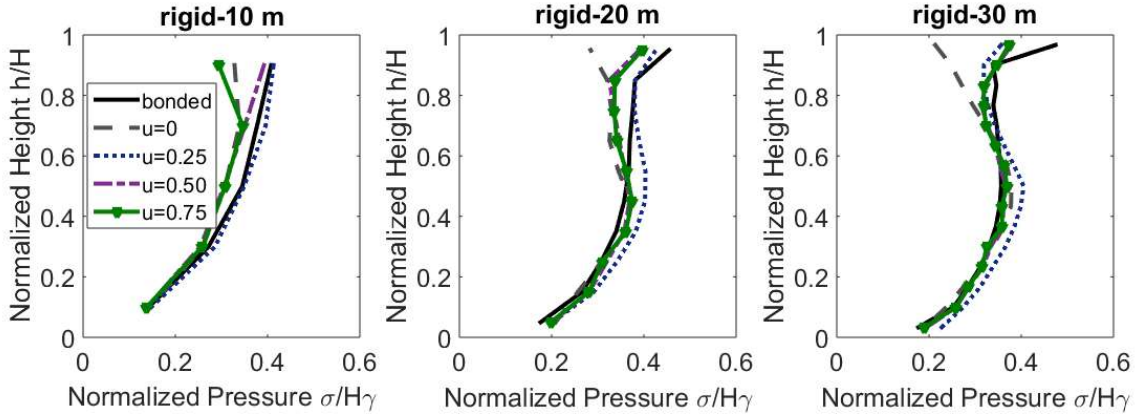

Figure 10: **Normalized seismic pressures for rigid walls (1000*E)**.

CONCLUSIONS

This study focused on the analysis of the seismic soil pressures developed on rigid and flexible embedded retaining walls when subjected to non-pulse seismic excitations with different contact friction conditions. A finite element model of a wall and surrounding soil was developed using Abaqus. The bonded condition was compared with models including friction between the soil and wall to assess the impact in the seismic soil pressures when different contact conditions are integrated. From the results, it was noticed that the distribution of the average seismic pressures is greatly affected by the wall flexibility. As the height of the wall increases, the change in pressure distribution is more noticeable. Changes in friction coefficients or bonded condition have in general mayor effects as the flexibility of the wall increases. These results indicate the importance of parameters like the wall flexibility and contact conditions in modelling the seismic response of these systems. If accurate representation of seismic pressures is the goal, these parameters cannot be overlooked. The conclusions of this study are limited by the assumptions and simplifications in the numerical model used. Further studies will include more earthquake records with different moment magnitudes to identify factors that are responsible for the result variability. Several wall heights will also be included to extend these analyses.

ACKNOWLEDGMENTS

This work was performed under award NRC-HQ-60-17-G-0033 from the US Nuclear Regulatory Commission. The statements, findings, conclusions, and recommendations are those of the authors and do not necessarily reflect the view of the US Nuclear Regulatory Commission.

REFERENCES

Abaqus. **(**2016**)**. Unified FEA. Dassault Systèmes.

Ancheta T.D., Darragh R.B., Stewart J.P., Seyhan E., Silva W.J., Chiou B.S.J., Wooddell K.E., Graves R.W., Kottke A.R., Boore D.M., Kishida T. (2013). "PEER NGA-West2 Database, PEER Report 013/03", Pacific Earthquake Engineering Research Center, University of California, Berkeley, California.

Bolisetti C. and Whittaker A.S. (2015). "Site Response, Soil-Structure Interaction and Structure-Soil-Structure Interaction for Performance Assessment of Buildings and Nuclear Structures". MCEER-15-0002, June 1015, 388 pp.

Datta D., Colleman J., and Varma A.H. (2018). "Comparative analyses of contact algorithms for interface modelling in non-linear soil structure interaction", Proceedings of the Eleventh U.S. National Conference on Earthquake Engineering.

Hashash YMA, Musgrove MI, Harmon JA, Groholski DR, Phillips CA, Park D. (2016). DEEPSOIL 6.1 - User Manual. Urbana, IL, Board of Trustees of University of Illinois at Urbana-Champaign.

Kondner, R. L., and J. S. Zelasko. (1963). "A hyperbolic stress–strain formulation of sands", Proceedings of the 2nd Pan-American. conference on soil mechanics and foundation engineering, Brazilian Association of Soil Mechanics, Silo Paulo, Brazil,289–324.

Livermore Software Technology Corporation (LSTC), LS-DYNA Keyword User's Manual, May 2014.

Luna-Tezna R., Spears R., and Montejo L.A. (2018). "Time domain finite element modelling of seismic pressures on rigid retaining walls". Proceedings of the Eleventh U.S. National Conference on Earthquake Engineering.

Lysmer J. and Kuhlemeyer A.M. (1969). "Finite dynamic model for infinite media", Journal of the Engineering Mechanics Division, ASCE; Vol. 95, pp. 859-877.

Matasovic N. (1993). "Seismic response of composite horizontally-layered soil deposits", Ph.D. Dissertation, University of California, Los Angeles.

Psarropoulos, P. N., Klonaris, G., and Gazetas, G. (2005). "Seismic earth pressures on rigid and flexible retaining walls", Soil Dynamics and Earthquake Engineering, Vol. 25, No. 7-10, pp. 795-809.

Roman-Velez X., and Montejo L.A. (2020). “Generation of seed-based spectrum-compatible pulse-like time-Series”. Bulletin of Earthquake Engineering, Vol. 18, No. 4, pp. 1161-86.

Wagner N. and Sitar N. (2016). “Seismic earth pressures on deep stiff walls”, Geotechnical and Structural Engineering Congress.

World Nuclear Association. (2021). “World Nuclear Performance Report 2021”.

Xu J., Miller C., Costantino C., Hofmayer C., and Graves H.L. (2006). “Assessment of seismic analysis methodologies for deeply embedded nuclear power plant structures”. U.S. Nuclear Regulatory Commission. NUREG/CR-6896/BNL-NUREG-754 10-2006.